Chapter 6

Estimating Cambro-Ordovician seawater temperature and isotopic composition using carbonate clumped isotope paleothermometry on calcitic and phosphatic fossils

Kristin D. Bergmann[1], Seth Finnegan[2], John Eiler[1] and Woodward Fischer[1]

[1]California Institute of Technology

[2]University of California, Berkeley

6.1 Abstract

A secular increase in δ^{18}O values of both calcitic and phosphatic marine fossils through early Phanerozoic time suggests three end-member hypotheses 1) surface temperatures during the early Paleozoic were very warm, in excess of 40°C (tropical MAT) [1], 2) the δ^{18}O isotopic composition of seawater has increased by up to 7–8‰ VSMOW over the Phanerozoic [2, 3, 4] or 3) ancient materials are more significantly altered via post-depositional diagenetic processes. Carbonate clumped isotope analysis, in combination with petrographic and elemental analysis, has the potential to differentiate between these hypotheses. A sample suite including both calcitic and phosphatic marine fossils, the first paired study of its kind, from

Cambrian- and early Ordovician-aged rocks indicate seawater temperatures were warmer than today (avg. 30-35°C. None of the fossil materials indicate seawater compositions as depleted in δ^{18}Oas some have suggested (-7‰) [2, 3, 4]. Additionally, recent phosphate-water equilibrium fractionation equations suggest mutual equilibrium precipitation for $\delta^{18}O_{CO3}$ and $\delta^{18}O_{PO4}$ from the same fluid [5, 6].

6.2 Introduction

Early isotopic measurements of ancient calcite [7], apatite [8] and chert [9, 10] documented a secular increase in the δ^{18}O of each mineral over Phanerozoic time. This trend suggests three end-member hypotheses 1) ocean temperatures have decreased since Precambrian time, 2) the oxygen isotopic composition of seawater has evolved through time or 3) diagenetic processes are more important in ancient samples. It has been difficult to evaluate these hypotheses because the δ^{18}O composition of rocks and fossils depends on both the precipitating temperature and the δ^{18}O of water. Diagenetic processes that modify geological materials can overprint primary isotopic signatures. However, the gradual mirrored decline in the δ^{18}O of three separate mineral phases with very different solubility behaviors over the course of Phanerozoic time suggest diagenetic alteration of older materials cannot explain the entire pattern. Determining the relative contributions of temperature and $\delta^{18}O_{seawater}$ change to the $\delta^{18}O_{min}$ records is critical to understanding the evolution of the early-Paleozoic climate and the diversification of animals.

Paired isotopic analysis of co-occurring sample suites of apatite and calcite [11, 12] or apatite and chert [9] provides a powerful approach to test mutual equilibrium fractionation of the different phases. However, results from previous paired studies have varied and interpretations of the trends are inconsistent. Some authors have postulated equilibrium precipitation of both phases suggestive of exceedingly warm ocean temperatures and no change in bulk fluid composition [9, 13] whereas other studies suggest one or more mineral phases are not precipitated in equilibrium from primary fluids leaving doubt as to whether the isotopic composition of the fluid has varied [14, 11, 12].

Another approach used to examine the long-term evolution of seawater δ^{18}O has been to examine the ophiolite record through time [15, 16, 17]. The record of hydrothermal alteration of basalts formed at mid-ocean ridges suggests the seawater composition has remained invariant since the Archean. Analytical results indicate a constant gradient in δ^{18}O of oceanic crusts through time where the pillow basalts are enriched (δ^{18}O $\sim$ 6–10‰ VSMOW) relative to concurrent gabbros (δ^{18}O $\sim$ 3–6‰VSMOW) indicating exchange with 0‰ VSMOW seawater at different temperatures (e.g., [17]). These results are supported by theoretical modeling of seawater exchange with basaltic crust at cooler temperatures in the pillow basalts and hydrothermally in the gabbroic deposits formed at mid-ocean ridges [15]. These exchange reactions along with subduction and recycling of saturated sediments have been argued to buffer and maintain seawater compositions of $\sim$ 0‰ if seafloor spreading rates are $\geq$0.5 times present rates [15, 16, 18].

More recently, higher resolution records of a single mineral phase have been used to argue for each end-member interpretation. δ^{18}O measurements of conodont apatite by secondary ion mass spectrometry (SIMS) have been used to suggest a decline of sea surface temperatures through the Ordovician from temperatures in excess of 40°C in the early Ordovician, which the authors postulate spurred the early Ordovician radiation of a wide variety of skeletalized calcitic taxa [1]. In contrast, records of the δ^{18}O of Paleozoic brachiopods have been used to suggest a secular change in the bulk isotopic composition of seawater to values reaching -7‰ in the early Paleozoic [2, 3, 19, 4, 20]. These large discrepancies in interpretation arise from different assumptions for the cause of the $\delta^{18}O_{min}$ decline.

Interpretations of previous δ^{18}O phosphate records [1] and paired phosphate-carbonate [11, 8, 13, 12] or phosphate-chert studies [9] have been thrown into doubt recently because the phosphate-water equilibrium fractionation equation is currently in a state of flux [21, 6]. Over the last 40 years, a variety of chemical methods and analytical tools were used to isolate and measure the δ^{18}O of PO_4. Chemical isolation methods precipitate either $BiPO_4$ or more recently tri-silver phosphate, Ag_3PO_4. These compounds are then measured by laser fluorination or with a Thermal Conversion Elemental Analyzer –Isotope Ratio Mass Spectrometer (TC/EA – IRMS). There is analytical evidence that these different precipitation and measurement methods do not yield consistent results [21, 6]. Because of these uncertainties there is also continued debate over the isotopic composition of the widely used standard NBS 120-C used to calibrate phosphate measurements [6].

Carbonate clumped isotope thermometry can constrain the interpretation of changing $\delta^{18}O_{min}$ through early Paleozoic time by providing an independent measure of crystallization temperature [22] and, when paired with classical $\delta^{18}O$ paleothermometry [23, 24], can determine the isotopic composition of the fluid the mineral last equilibrated with (not limited to seawater but including diagenetic pore fluids and formation waters). Combined with petrographic and elemental analysis, this method has the potential to untangle primary isotopic signatures from diagenetic signals.

Here we develop a paired phosphate-calcite record using carbonate clumped isotope thermometry for the Cambrian and Ordovician, the interval with the most significant change in $\delta^{18}O_{min}$. This approach has the benefit of measuring the clumped isotope distribution in two minerals that have different susceptibilities to diagenetic dissolution. Phosphatic materials also provide an archive prior to the rise of thick-shelled calcitic fossils during the Ordovician radiation.

We measured the carbonate clumped isotopic compositions (Δ_{47} values) of carbonate ion units substituted into the phosphate lattice of phosphatic inarticulate brachiopods in Cambrian and Ordovician strata and calcitic brachiopods, trilobites, rugose corals and carbonate mud from Ordovician strata. We also compared measurements of the $\delta^{18}O$ of CO_3 groups with the $\delta^{18}O$ of PO_4 groups from the inarticulate brachiopods to test whether the carbonate clumped isotope measurements yield mutual equilibrium fractionation and are thus consistent with primary growth temperatures. To build on previous phosphatic calibration studies of carbonate clumped isotope thermometry in dentin and enamel of bone and teeth [25, 26], we calibrate this tool by measuring the clumped isotope values

(Δ_{47}) of CO_2 extracted from modern inarticulate phosphatic brachiopods of known growth temperatures.

6.3 Geologic Setting

6.3.1 Modern samples

Modern inarticulate brachiopod samples were provided by the L.A. County Museum of Natural History and the Waikiki Aquarium from well constrained locations. To best calibrate the measurements in modern samples, shells grown in a range of mean average temperatures were selected. The sample suite includes valves of *Glottidia albida* from Terminal Island and Newport Bay, CA, *Lingula reevii* (raised in the Waikiki Aquarium for $>$ 5 years after being harvested from Kaneohe Bay, Hawaii), *Lingula ungis* from the Polillo Islands, Philippines and *Glottidia pyramidata* from Tampa Bay, Florida. One specimen of a calcitic brachiopod *Terebratalia transversa* from the San Pedro Jetty was also analyzed for a paired analysis of calcite and phosphate shell materials from nearby localities. Measurements are compared to minimum, maximum and mean sea surface temperatures over the last 5-10 years from nearby ocean buoys and $\delta^{18}O_{seawater}$ values from GISS monitoring sites (Fig. 6.2) [27].

6.3.2 End Ordovician- to Silurian-aged Anticosti and Cincinnati Series

The sedimentology and locations of the calcitic fossil materials published in [28, 29] are described in the supplemental materials for each publication. Samples were primarily from Anticosti Island, Quebec as well as the Cincinnati Series of Kentucky and Ohio [28].

6.3.3 Decorah Formation

The Late Ordovician Decorah Formation (Mowhawkian) in the Upper Mississippi Valley region is a mixed carbonate-siliciclastic unit deposited in the Hollandale

Embayment [30, 31]. The Decorah Formation has multiple features that make it an ideal target for this study. The unit is host to four bentonite ash deposits, the Deicke, Millbrig, Elkport and Dickeyville beds, that can be correlated across North America and potentially to Europe [32]. The Decorah Formation also includes the Guttenberg Carbon Isotope Excursion (GICE) that has been suggested to have similar forcing mechanisms as the Hirnantian Isotope Excursion (HICE) [33, 31, 34]. The Upper Mississippi Valley Decorah Formation has seen minimal burial although sections further to the south in Wisconsin show evidence for Mississippi Valley Type alteration.

The lithology varies from poorly lithified mixed carbonate muds and illite clays to fossiliferous packstone beds that developed hardground features including extensive burrowing by *chondrites* [30]. The Decorah Formation likely had low sedimentation rates, as it was deposited during one of the largest transgressions on the North American craton [30]. This is evidenced by phosphatized grains in the lower Decorah Formation, iron ooids which appear in the more northerly sections in Minnesota and abundant hardgrounds [31, 30]. The abundant brachiopods, rugose corals, trilobites, crinoids and bryozoa including *prasaspora* provide a rich selection of different fossil materials to analyze. Additionally, in the Ion Member overlying the Guttenberg Member, abundant large inarticulate brachiopods, *Lingulasma galenaense*, can be found near Decorah, Iowa at the Decorah Bruening Quarry and Pole Line Road localities. These phosphatic fossils allow for a paired analysis of calcitic and phosphatic materials from the same horizon.

6.3.4 Volkhov, Kunda and Aseri Stages

The stratigraphy capturing the Volkhov, Kunda and Aseri Stages (equiv. to Arenig and Llanvirn) of Estonia and St. Petersburg, Russia are one of the few sections globally that preserves abundant calcitic fossil materials with minimal burial history from Lower-Middle Ordovician aged rocks. Fossils from the Baltic-Ladoga Glint, an escarpment, are found within limestone wackestone and packstone beds as well as in the unlithified clay-rich interlayers [35, 36]. The total thickness of Ordovician stratigraphy is 100-200 meters thick. The Volkhov Formation is the first carbonate rich formation overlying predominantly quartz sand and clay lithologies of Cambrian and early Ordovician age. It was deposited on a broad epicontinental shelf with low sedimentation rates and is 12 meters thick [37, 38]. Hardgrounds are abundant, the sediments tend to be glauconiferous and the ooids are ferruginous [38, 37, 39]. The Kunda and Aseri stages of the Baltic-Ladoga Glint ($\sim$ 12 meters total thickness) are known for their abundant and excellently preserved trilobite fauna [37]. Iron ooids and glauconite grains remain an important component of these sediments. Mud mounds $\sim$ 3–4 meters in height and 100–200 meters in diameter are also a component of the depositional environment [37, 38].

6.3.5 Eau Claire Formation

The Upper Cambrian-aged Eau Claire Formation of Wisconsin and Minnesota was one of the first Cambrian sandstones deposited on the craton in these localities. The sandstones in Wisconsin are generally coarse grained quartzose-feldspathic sandstones with well-rounded grains and are thought to be from a nearshore environment [40]. These nearshore siliciclastics grade into carbonates in Iowa.

The Eau Claire Formation preserves the Steptoean Positive Carbon Isotope Excursion (SPICE) in carbonate lithologies in Iowa [41, 42]. A study of the abundant inarticulate brachiopods found in the Eau Claire recovered the SPICE excursion in the CO_3 groups substituted into the phosphate lattice. The inarticulate brachiopods recover the SPICE with δ^{13}C values identical to the surrounding carbonate matrix and other global sections recording the SPICE [40]. Interestingly, the δ^{13}C of the CO_3 from the inarticulate brachiopods recovered from the near shore sand dominated sediments in Wisconsin are offset by about -5‰ for the entire excursion. A reasonable explanation for this offset is the nearshore sandy environment in Wisconsin was estuarine and the DIC in the environment was isotopically light because of mixing with terrestrial light carbon. This is supported by the δ^{18}O of the CO_3 groups measured from the two populations. In general the δ^{18}O is lighter in the inarticulate brachiopods from Wisconsin by $\sim$ 4‰likely from more brackish water [43].

The different localities sampled for this study are all from the siliciclastic dominated nearshore environment because sample size limitations currently make subsurface core sampling of the more offshore deposits problematic. The collection sites are near Strum and Colfax, Wisconsin and have different dominant genera of *Lingulepis* and span two trilobite zones *Cedaria* and *Crepicephalus*.

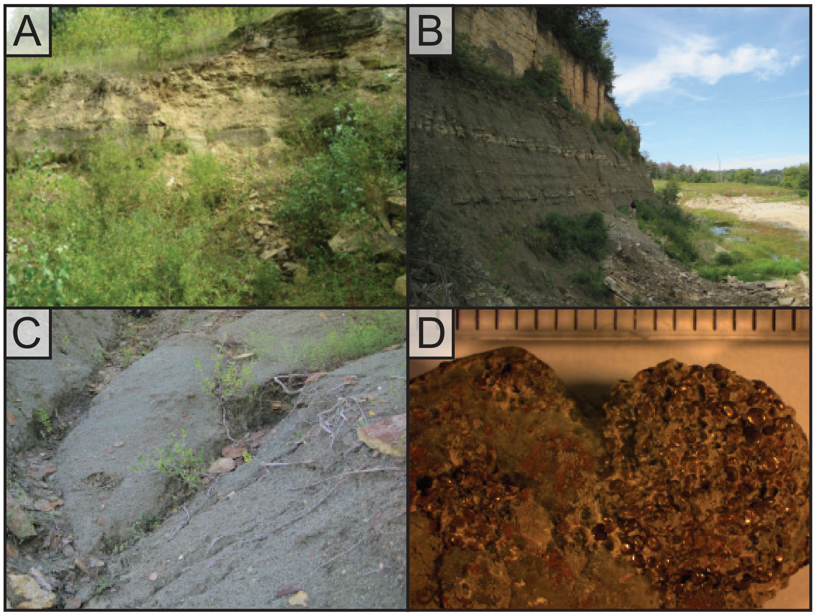

Figure 6.1: Field photographs of the Eau Claire and Decorah Formations. a. Sandstone lithology of the Eau Claire Formation near Strum, Wisconsin. b. Mixed poorly lithified mudstone and cemented packstone carbonate lithologies of the Decorah Formation at the Decorah Bruening Quarry, Decorah, IA. c. Mineralized hardground surfaces with significant burrowing interbedded with poorly lithified mudstone near Rochester, MN. d. Abundant iron ooids from the middle Decorah Formation near Rochester, MN.

6.4 Methods

6.4.1 Sample collection and preparation

Samples of calcitic fossil materials including articulate brachiopods, rugose corals and trilobites were collected from six locations of the fossiliferous Decorah Formation in Minnesota, Iowa and Wisconsin in the summers of 2010 and 2011. Phosphatic inarticulate brachiopods were collected from a horizon of the Ion Member in the Decorah Bruening Quarry. Calcitic brachiopods from the lower part of the Volkhov Formation were collected by P. Fedorov and provided by L. Popov. Trilobites and carbonate wackestone matrix were also acquired from the Russian Asery and Kunda Formations. Phosphatic inarticulate brachiopod material was collected from the Eau Claire Formation from five localities in Wisconsin in the summer of 2011.

Once extracted from the bulk sediments, calcitic and phosphatic taxa were washed and sonicated in DI water to remove loose sediment. Additional physical cleaning was completed on all taxa using dental picks, a toothbrush and sand abrasion. Calcitic brachiopod shells were gently crushed and picked for flakes preserving the fibrous secondary layer while the recrystallized primary layer was avoided as best as possible. These individual fragments were then powdered in a mortar and pestle. Trilobite fragments not contaminated with carbonate mud were crushed and powdered. Rugose corals were sectioned in two directions and a small portion of skeletal material was drilled, avoiding visible borings.

Phosphatic inarticulate brachiopod shells were isolated from the siliciclastic rich sediments of the Eau Claire using a dremel, sonication in DI water and sand abrasion. Phosphatic shells from the Decorah Formation were isolated from the carbonate fraction using a weak acetic acid solution (10%). A 'sample' of many inarticulate brachiopod fragments was then powdered and treated with a range of cleaning solutions to target organic material including: none, 3% H_2O_2 for 4 hours, 30% H_2O_2 for 24 hours, 50–50 30% H_2O_2 and 3% NaOCl for for 24 hours, and 50-50 30% H_2O_2 and 1M NaOH until no reaction was visible. All powders were then treated with a 0.1 M buffered acetic and acetate solution for 12 hours to remove labile CO_3 groups [44].

6.4.2 Carbonate clumped isotope thermometry

Samples were analyzed over the period of December, 2010-Jan, 2013. 9–12 mg of calcitic powder or 100-200 mg of phosphatic powder was weighed into silver capsules before being reacted at 90°C in 100% H_3PO_4 in a common acid bath.

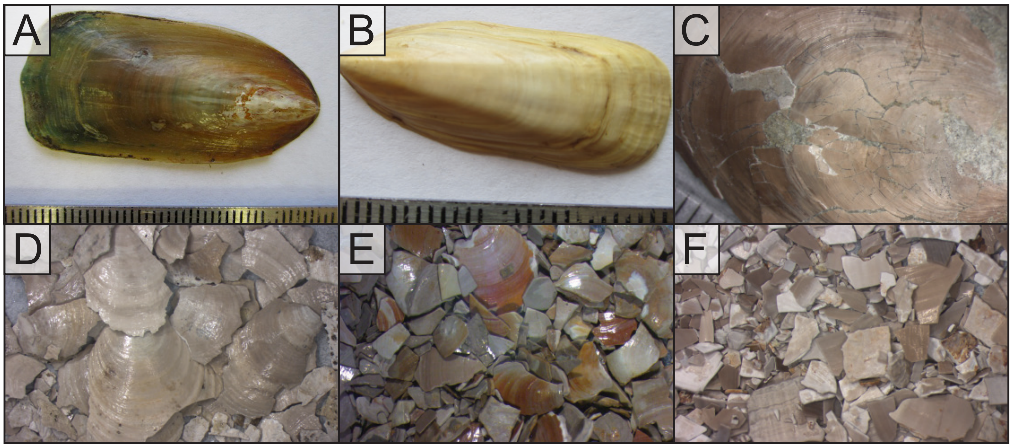

Figure 6.2: Modern and ancient inarticulate brachiopod samples. a. *Lingula unguis* from the Polillo Islands, Philippines b. *Glottidia albida* from the San Pedro shelf off San Pedro, CA. c. *Lingulasma galenaense* recovered from the Ion Member of the Decorah Formation at the Decorah Bruening Quarry. d. prepared sample of *Lingula sp.* from the *Crepicephalus* zone of the Eau Claire Formation near Colfax, WI. e. prepared sample of *Lingula sp.* from the *Crepicephalus* zone of the Eau Claire Formation near Strum, WI.

Evolved CO_2 was purified by multiple cryogenic traps including a Porapak-Q chromatograph held at -20°C before being measured on a ThermoFinnigan MAT 253 IRMS. Methods for the measurement and corrections to analyzed heated gases run during each session following [45, 46]. After corrections based on the heated gas line from a given session and an intercept shift based on the initial calibration experiment, Δ_{47} values were transformed into an absolute reference frame using a secondary transfer function following [47, 48]. The secondary transfer function for each week was calculated using any of the following available data: 25°C and 1000°C CO_2 as well as any of four carbonate standards with known absolute reference frame values (see below). Finally Δ_{47} values for carbonate samples were corrected by $+0.092‰$ for the 90°C acid bath reaction temperature within the absolute reference frame [48].

Values of Δ_{47} within the absolute reference frame (ARF) for two internal standards used over the course of the analyses, Yale CM (n=35) and TV01 (n=50) were calculated from 7 weeks when 1000°C CO_2 was analyzed daily and 25°C CO_2 gases were analyzed bi-weekly. The calculated values for the two standards in the absolute reference frame are reported with 1 SD for all sessions with heated gases and equilibrated gases: Yale CM (n = 33) Δ_{47}-ARF = 0.404 ± 0.022‰, TV01 (n = 50) Δ_{47}-ARF = 0.730 ± 0.018‰. Absolute reference frame values for two other internal standards run during the analytical period were calculated from weeks where either Yale CM and/or TV01 had been run with them (GC-AZ-01 (n=12) and Carmel Chalk (n=15)). Values are reported with 1 SD for all sessions with heated gases and known standards: 102-GC-AZ01 (n = 12) Δ_{47}-ARF = 0.709 ± 0.023‰, and Carmel Chalk (n=15) Δ_{47}-ARF = 0.678 ± 0.020‰. The values of the Carrara standard and 102-GC-AZ01 in the absolute reference frame are nearly identical to those found at Johns Hopkins (UU Carrara (n = 93) Δ_{47}-ARF = 0.403 ± 0.015‰ and 102-GC-AZ01 (n = 102) Δ_{47}-ARF = 0.710 ± 0.015‰ [48].

The reproducibility of standards for all analytical weeks are reported with 1 SD for all sessions: Yale CM (n = 98) Δ_{47}-ARF = 0.405 ± 0.019‰, 102-GC-AZ01 (n = 23) Δ_{47}-ARF 0.710 ± 0.011‰, TV01 (n = 86) Δ_{47}-ARF 0.730 ± 0.015‰ and Carmel Chalk (n = 17) Δ_{47}-ARF 0.675 ± 0.015‰. For single unknown measurements the uncertainty of the measurement is reported as the standard error of the mean (SEM) of Δ_{47} measurements over 8 acquisitions. For $n \geq 2$, the error is reported as the SEM of Δ_{47} over the number of sample replicates.

Temperatures were calculated in the absolute reference frame as well as the interlab reference frame using the same calibration data from two calibration studies completed at Caltech [49, 50]. To build this calibration equation from low to high temperatures we assume that calcite and dolomite calibrations are equivalent. The two approaches do not yield the exact same temperature on a week to week basis and this is likely due to two factors: 1) conversion of the two calibration studies into the absolute reference frame is imperfect because the samples were analyzed before 25°C CO_2 gases were analyzed regularly and 2) Converting unknown samples into the absolute reference frame using both gases and carbonate standards in the transfer function will correct for standard residuals for a given week.

The $\delta^{18}O_{min}$ composition was calculated using a 90°C acid digestion fractionation factor [51]. Fluid compositions were calculated using the measured clumped isotope temperatures and an equilibrium fractionation equation for calcite-water [24].

For the phosphatic brachiopod data, given the close agreement of previous calibration datasets [25] and ours (see below), we used the calcite and dolomite calibration studies generated at Caltech [49, 50] to calculate clumped isotope temperatures. To calculate $\delta^{18}O_{water}$ compositions, we assumed the equilibrium fractionation of the CO_3 groups follows calcite-water equlibrium fractionation [24]. This assumption is supported by the close agreement with local water compositions in our modern calibration dataset.

6.4.3 Phosphate oxygen isotope measurements

The $\delta^{18}O_{PO4}$ of four samples was analyzed by Ken MacLeod at the University of Missouri. The cleaned powders of inarticulate brachiopods from two modern locations (Southern California and the Polillo Islands, Philippines), the Decorah and Eau Claire formations where dissolved in dilute hydrofluoric acid. Ag_3PO_4 was precipitated from the solution using a silver amine solution where excess Ag^+ was added as $AgNO_3$. The pH was then increased using NH_4OH buffered with NH_4NO_3 and samples were left uncovered at $\sim$ 50°C. Ag_3PO_4 precipitates slowly out of solution as the pH decreases. The silver phosphate crystals were rinsed, dried and stored in a desiccator prior to being weighed into silver capsules. The capsules were then combusted in a high temperature ($\sim$ 1400°C) TC/EA before being analyzed as CO on an IRMS. The isotopic measurements are reported relative to VSMOW and analytical precision is $\leq \pm 0.3$‰.

6.4.4 SEM/electron microprobe

A ZEISS 1550 VP Field Emission Scanning Electron Microscope (SEM) equipped with an Oxford INCA Energy 300 x-ray Energy Dispersive Spectrometer (EDS) system within the California Institute of Technology Geological and Planetary Sciences Division Analytical Facility was used for high-resolution imaging of each sample. Images were collected at a working distance between 7–9 mm using a Quadrant Back Scattering Detector (QBSD).

Quantitative elemental spot analysis and elemental mapping on the fossil materials to assess trace metal variability on the micro-scale was conducted on the JEOL JXA-8200 Electron Microprobe. For all quantitative results, the accelerating voltage was 15 kV, the beam current was 20 nA, and the beam size was 1 μm. The CITZAF method was used for matrix correction. Sample standards for the five chemical elements analyzed on calcitic samples, included: calcite for Ca, dolomite for Mg, siderite for Fe, rhodochrosite for Mn, strontianite for Sr, and anhydrite for S. Ca had an average detection limit of 161 ppm, Mg–294 ppm, Fe–312 ppm, Mn–293 ppm, Sr–507 ppm, and S–91 ppm. Sample standards for the ten elements mapped on the apatite inarticulate brachiopod included: anhydrite for S, apatite for P, cerium phosphate for Ce, albite for Na, fluorine mica for F, apatite for Ca, yttrium phosphate for Y, dolomite for Mg, siderite for Fe, and strontianite for Sr.

6.4.5 Bulk powder inductively coupled plasma optical emission spectroscopy (ICP-OES)

An aliquot of powder from many of the calcitic clumped isotope samples was analyzed for trace metals on an ICP-OES (n = 63 of 130). Between 1–3 mg of powder was dissolved in 3 mL of dilute nitric acid for 24 hours at 25°C at the California Institute of Technology. Samples were analyzed at the Jet Propulsion Laboratory using a Thermo iCAP 6300 radial view ICP-OES with a Cetac ASX 260 autosampler with solutions aspirated to the Ar plasma using a peristaltic pump. Three standard solutions of 10 ppb, 100 ppb and 1 ppm of Fe, Mn, and Sr were run between every 8 sample unknowns. A methods blank was also analyzed during the analytical run.

6.4.6 Bulk powder x-ray diffraction (XRD)

XRD measurements were made on powders of the inarticulate brachiopod materials used for clumped isotope measurements on a PANalytical X'Pert Pro within the Material Science at the California Institute of Technology. Scans were run from 5–70° 2θ with a step size of 0.008 and a scan step time of 10.16 s. A Cu anode was used at 45 kV and 40 mA. A zero-background silicon plate was used for all measurements because of sample size limitations. Mineralogical phases that most closely matched a given inarticulate brachiopod sample were identified using the X'Pert Highscore IDMin function.

6.5 Results

6.5.1 Modern inarticulate brachiopod calibration

The modern inarticulate brachiopods used for calibration were from both extant genera of inarticulates—*Lingula* and *Glottidia*—from four locations worldwide, Tampa Bay, Florida, Newport Bay and Terminal Island, Southern California, Waikiki Aquarium, Hawaii, and the Polillo Island, Philippines. The SEM images of the shells indicate a wide range of phosphatic microstructure morphologies from the more massive structure in the mineralized primary layers to elaborate cross-hatching and vertical growth structures in the organic-rich, chitinous layers (Fig. 6.4). XRD analysis of modern inarticulate shell powders indicate the calcium phosphate has significant amounts of CO_3 and F substituted into the lattice and is most similar to the minerals Francolite $CaF(Ca, C)_4[P,C(O,OH,F)_4]_3$, Carbonate-Fluorapatite $Ca_{10}(PO_4)_5CO_3F_{1.5}(OH)_{0.5}$ and Hydroxyapatite $Ca_5(PO_4)_3(OH)$.

Clumped isotope analyses following treatment in a 0.1 M buffered acetic and acetate solution for 12 hours [44] were depleted in δ^{13}C, δ^{18}O, and Δ_{47} and enriched in Δ_{48}, suggesting organic material is likely both decarboxylating in the phosphoric acid and providing isobaric interferences. A variety of cleaning methods were compared to target the significant amount of organic material present in modern inarticulate shells [44]. Most of the organic material is gone from the fossil shells and a range of cleaning methods yielded consistent results. The most aggressive cleaning methods were the only reliable option to fully remove the $\sim$ 40 wt.% organic material (Fig. 6.3). After aggressive cleaning and a 12 hour treatment in a 0.1 M buffered acetic and acetate solution, the modern inarticulate brachiopods yielded temperatures and calculated seawater compositions within error of nearby NDBC buoy temperatures and gridded δ^{18}O seawater values from WOCE (Fig. 6.3) [27]. These phosphatic samples are in good agreement with previously analyzed calcite and phosphatic calibration materials [25, 50, 52, 53]. The $\delta^{18}O_{PO4}$ of the modern inarticulates is in isotopic equilibrium with the $\delta^{18}O_{CO3}$ of the most aggressively cleaned samples, where the clumped isotope temperature can be used to calculate water compositions from the two separate $\delta^{18}O_{min}$ measurements. Recent PO_4-water equilibrium equations are better predictors than older equations (Table 6.2) [6, 5].

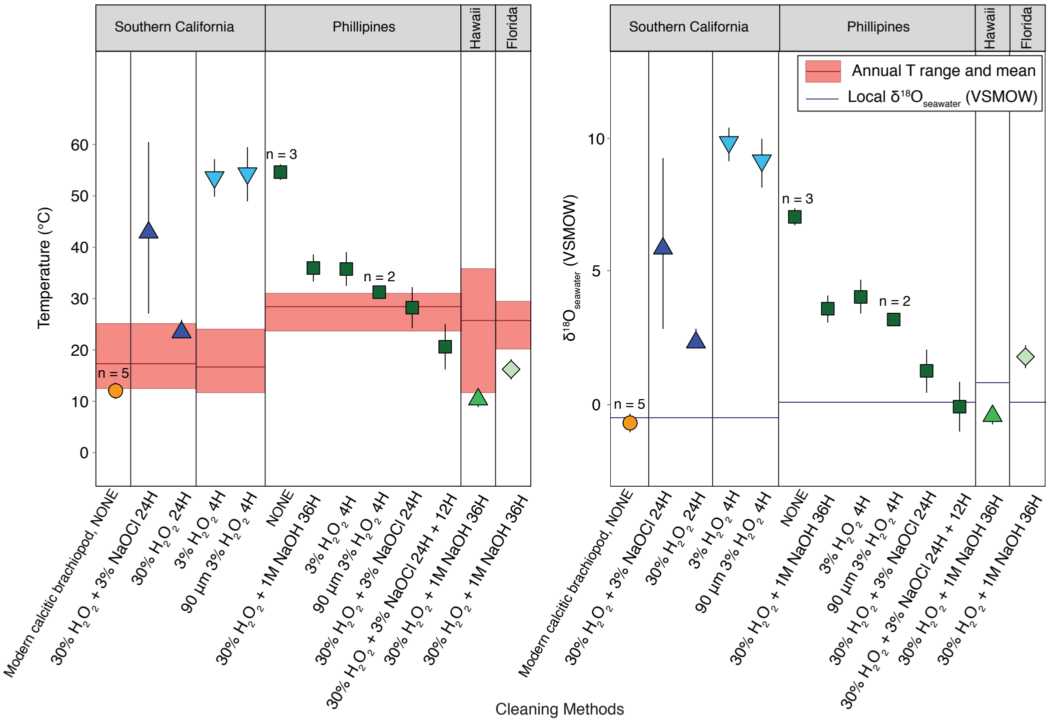

Figure 6.3: Modern inarticulate brachiopod clumped isotope calibration. left, clumped isotope temperature measured compared to min, max and mean temperature from the closest buoy in NODC. A variety of cleaning methods were tried as the uncleaned samples produced depleted Δ_{47} values relative to expected. right, calculated $\delta^{18}O_{water}$ compositions compared to the closest GISS measurements.

references for GISS data [27] and water calculations [24]

6.5.2 Decorah Formation

The calcitic brachiopods from the Decorah Formation display exceptional preservation of their secondary layers. The regular plates (Fig. 6.4c,e) look very similar to the plates of the secondary layer of a modern calcitic brachiopod *Terebratalia transversa*, recovered from the San Pedro Jetty, CA (Fig. 6.4a,b). However, in many of the calcite brachiopod shells examined on the SEM the massive primary layer has a recrystallized appearance and this region of recrystallization often spreads into the well-preserved secondary layer (Fig. 6.4d,f). The trace metal incorporation in the calcitic taxa of the Decorah Formation is of a very different character than that seen in the younger calcitic taxa analyzed in previous studies that span the end-Ordovician glaciation (Fig. 6.9) [28, 29]. The younger calcitic taxa including brachiopods, rugose corals and trilobites usually do not show significant enrichments in Fe^{2+} or Mn^{2+}. In contrast the calcitic taxa from the Decorah Formation show significant metal enrichments that are well outside of the field of modern metal incorporation in biogenic materials. Elemental maps and spot analyses along a shell transect for an example of a calcitic brachiopod from the Decorah Formation indicate Fe^{2+} enrichment. The punctae are filled with pyrite and a zone of dissolution and pyritization of the shell has spread out from the punctae. In the region of alteration Fe concentrations can be as high as 5500 ppm. Outside of the zone of alteration the Sr levels are high and Mn and Fe concentrations are low and look more similar to younger brachiopod materials (Fig. 6.5b,f,j,n,r). The inarticulate brachiopod species *Lingulasma galenaense* from the Decorah Formation shows similar microstructure as the modern inarticulate brachiopods. Both the massive mineralized layers are present as are the fine-scale cross hatched phosphatic precipitates in the chitinous layers. That said, the structures in both the modern and fossil inarticulate brachiopods are of a style that make it more challenging to visually identify whether recrystallization of the phosphate has occurred. XRD analysis of the *Lingulasma galenaense* samples from the Decorah Formation yielded spectra similar to the modern inarticulate brachiopod spectra and were most similar to the minerals Carbonate Hydroxyapatite $Ca_{10}(PO_4)_3(CO_3)_3(OH)_2$

and Francolite $CaF(Ca, C)_4[P,C(O,OH,F)_4]_3$.

Despite the general trend of increased Fe and Mn incorporation in the calcitic taxa from the Decorah Formations compared to the younger Ordovician and Silurian fossils analyzed in previous studies (Fig. 6.9) [28, 29], the clumped isotope results are remarkably similar. The lowest recorded temperatures from Decorah Formation samples are 35-36° ± 2°C, with one unreplicated sample from the GICE of 27° ± 2°C. The calculated $\delta^{18}O_{water}$ compositions for these low-end temperatures are -0.8 - -0.3 ± 0.2‰ VSMOW. Results from replicate clumped isotope analyses of the CO_3 groups substituted into the phosphate lattice of the inarticulate brachiopods from the Decorah Formation yielded temperatures of 40-42° ± 3°C. The calculated $\delta^{18}O_{water}$, assuming an equilibrium relationship that follows calcite [24], is 0.09 - 0.4 ± 0.5‰ VSMOW. These results overlap with the range of temperatures and fluid compositions of calcitic taxa including calcitic brachiopods, rugose corals, trilobites and matrix measured from the same site indicating these two minerals are not significantly different (Fig. 6.6). However, the lowest temperatures of 35-36°C recorded from some of the calcitic brachiopods and sieved $<$ 100 μm unconsolidated mud (lower blue circle in Fig. 6.6) suggest there is more potential for some alteration phases to be measured in the cemented carbonate nodules (higher blue circle in Fig. 6.6), rugose corals and trilobites.

6.5.3 Volkhov, Kunda and Aseri Stages

Electron microprobe maps and spot analyses of a brachiopod from the Volkhov Formation indicate it is enriched in Mn^{2+} within specific horizons in the shell material that follow the orientations of original plates in the secondary layer. Mn enrichments can be as high as 8000 ppm (Fig. 6.5a,e,i,m,q). The trilobite from the Aseri Stage shows two aspects suggesting diagenesis has altered the original material. The first is the even, high enrichment in Fe across the thickness of the shell to values over 3000 ppm. The second is the large dolomite rhombs that are ingrown at the sediment-shell interface (Fig. 6.5c,g,k,o,s).

The lowest temperatures of 32-33° ± 2°C from brachiopods from the Early

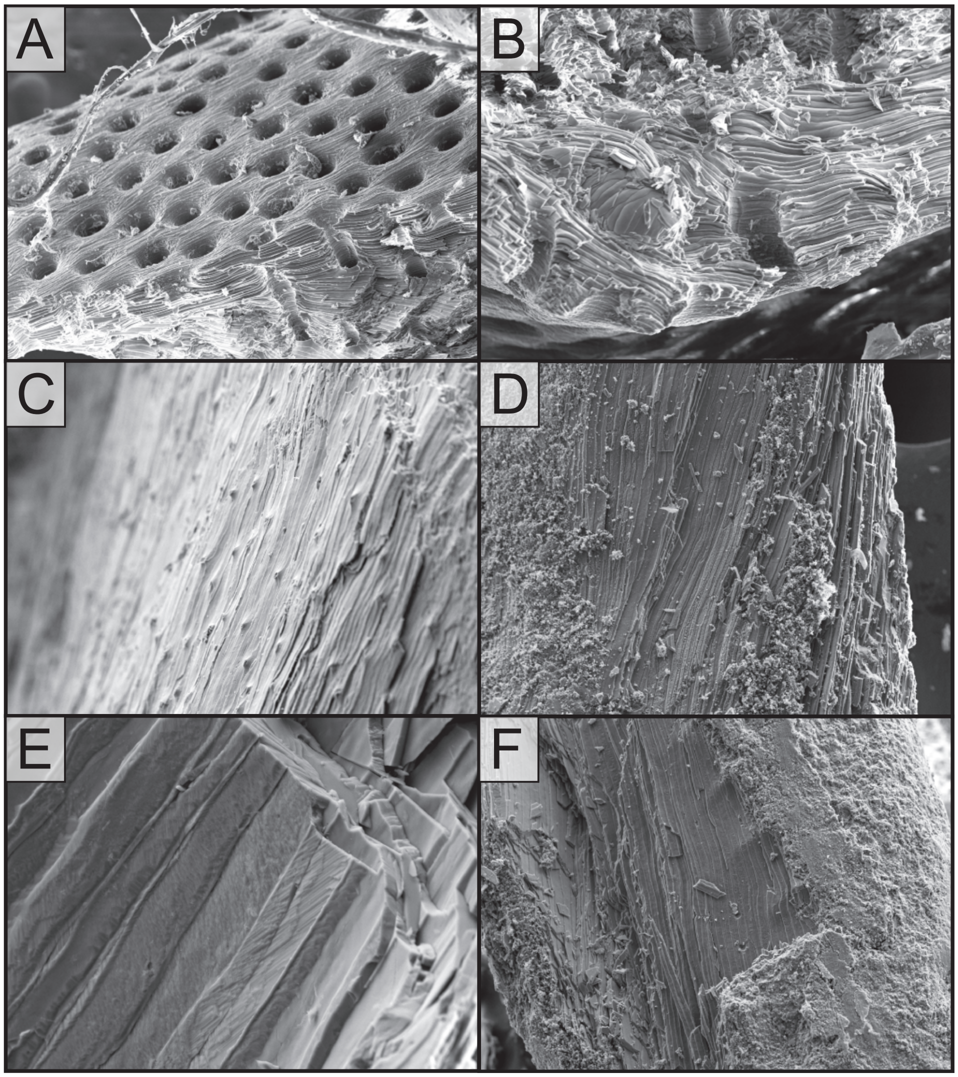

Figure 6.4: SEM images of modern and ancient articulate brachiopods. (a) & (b) shell structure of *Terebratalia transversa* from the San Pedro Jetty, CA. Note the abundant punctae. (c) & (e) Well-preserved calcitic brachiopods from the Decorah Formation (d) & (f) recrystallized primary layer with a well-preserved secondary layer in calcitic brachiopods from the Decorah Formation.

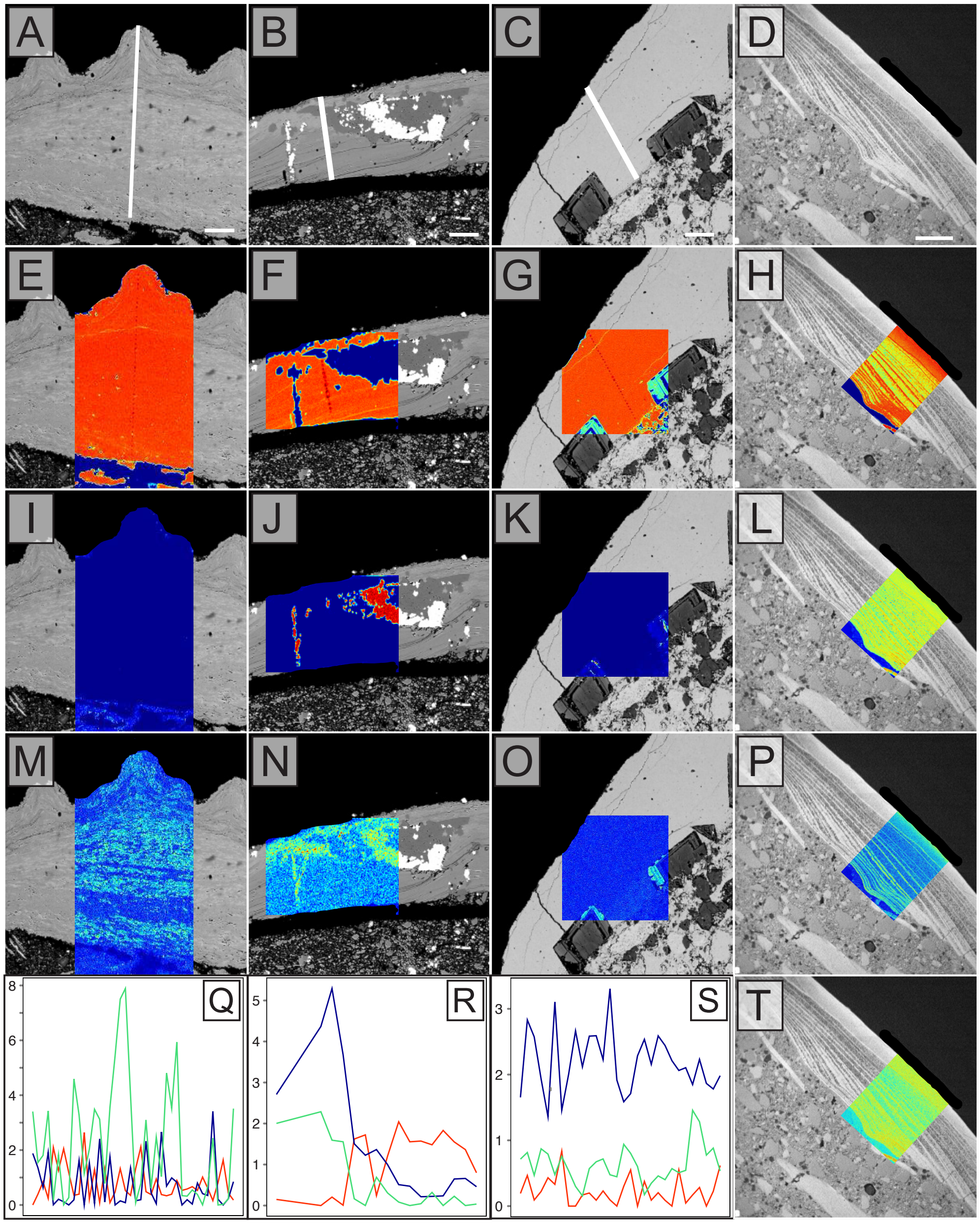

Figure 6.5: Electron microprobe maps and spot analyses of ancient brachiopods. (a) Calcitic brachiopod from the Volkhov Formation with overlain elemental maps generated on an electron microprobe of Ca (e), Fe (i), & Mn (m) and quantitative spot measurements (q) along a transect shown in (a). Scale bar is 110 μm. (b) Calcitic brachiopod from the Decorah Formation with overlain elemental maps of Ca (f), Fe (j), & Mn (n) and quantitative spot measurements (r) along a transect shown in (b). Scale bar is 60 μm. (c) Calcitic trilobite from the Asery Formation, Russia with overlain elemental maps of Ca (g), Fe (k), & Mn (o) and quantitative spot measurements (s) along a transect shown in (c). Note the ingrown dolomite rhombs along the base of the shell. Scale bar is 110 μm. (d) Phosphatic brachiopod from the Eau Claire Formation with overlain elemental maps of P (h), F (l), Na (p), & Ce (t). Scale bar is 200 μm.

Ordovician Volkhov Formation and trilobites from the Early-Middle Ordovician Aseri and Kunda Stages are slightly lower than the temperatures from the Decorah Formation and other Late Ordovician sections [28]. The calculated $\delta^{18}O_{water}$ compositions for the lowest temperature samples are -1.4 - -1.5 ± 0.5‰. Despite the significant amount of reduced trace metals (Fe, Mn) incorporated into the fossil materials and matrix of the Volkhov, Asery and Kunda materials, the maximum temperature measured of 41° ± 5°C is significantly lower than the maximum temperatures recorded in younger Ordovician and Silurian sample suites(Fig. 6.9) [28, 29].

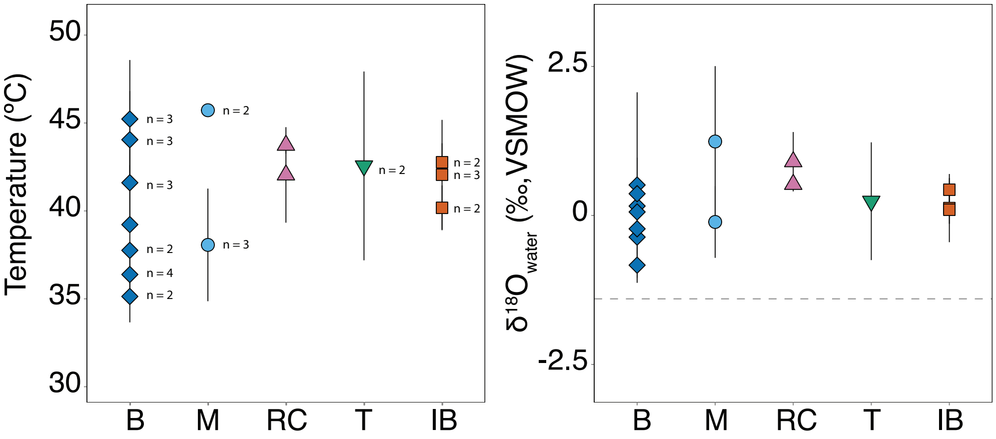

Figure 6.6: Single bed comparison of calcitic and phosphatic taxa from the Decorah Formation. left, clumped isotope temperatures measured for each taxa. right, calculated $\delta^{18}O_{water}$ compositions with the dashed line at predicted modern ice-free conditions. B – calcitic brachiopod, M – mud (lower = unconsolidated, upper = lithified), RC – rugose coral, T – trilobite, IB – inarticulate (phosphatic) brachiopod

reference for water calculation [24]

6.5.4 Eau Claire Formation

The *Lingula sp.* from the Cambrian Eau Claire Formation sampled near Colfax, WI are relatively thin, white in color and in some cases have lost all luster in the outer shell and appear powdery (Fig. 6.2d). In contrast the *Lingula sp.* from Strum, WI display brown color banding and are generally thicker (Fig. 6.2e). Few of the shells from the Strum site appear powdery. The inarticulate brachiopods *Lingula sp.* have very similar microstructures to both the Decorah

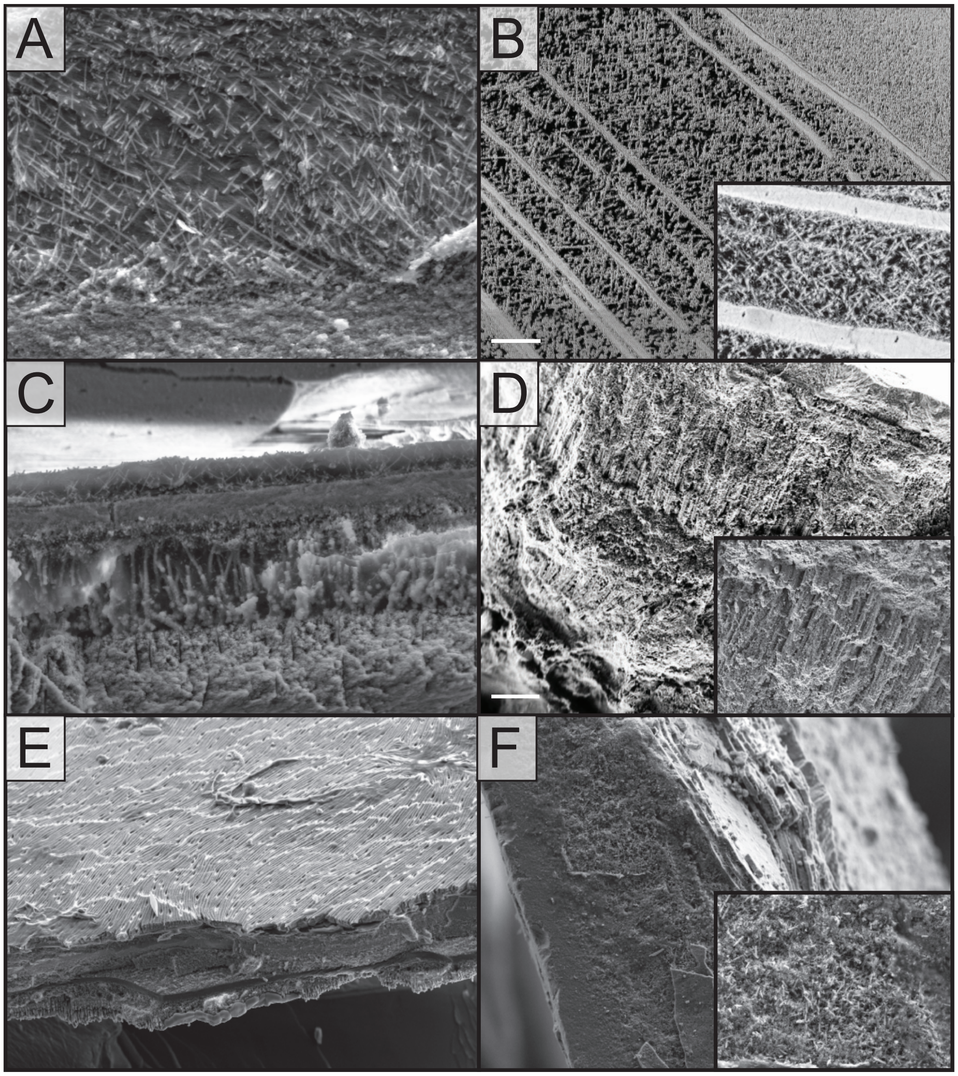

Figure 6.7: SEM images of modern and ancient inarticulate brachiopods. (a) & (c) shell structure of the secondary layer of a modern inarticulate brachiopod, *Glottidia albida* from the San Pedro shelf off Newport Bay, CA. (d) shell structure of a modern inarticulate brachiopod, *Lingula reevii* from the Waikiki Aquarium. (b) structure of the secondary layers in *Lingula sp.* recovered from the *Crepicephalus* zone of the Eau Claire Formation near Strum, WI. Scale bar is 20 μm. (d) structure of the secondary layers in *Lingula sp.* recovered from the *Crepicephalus* zone of the Eau Claire Formation near Colfax, WI. Scale bar is 40 μm. (f) shell structure of *Lingulasma galenaense* from the Decorah Formation collected from the Decorah Bruening Quarry, IA.

and modern inarticulate brachiopod species. The more porous organic-rich layers have cross-hatching and vertical phosphate precipitates (Fig. 6.7b,d). The XRD spectra are similar to the modern inarticulate brachiopod spectra and are close matches to the minerals Francolite CaF(Ca, C)$_4$[P,C(O,OH,F)$_4$]$_3$, Hydroxyapatite $Ca_5(PO_4)_3(OH)$, and Carbonate Hydroxyapatite $Ca_{10}(PO_4)_3(CO_3)_3(OH)_2$. The spectra also indicate that while not all of the quartz sand was removed from each powder prior to analysis there was no calcite or dolomite within the samples analyzed (Fig. 6.8).

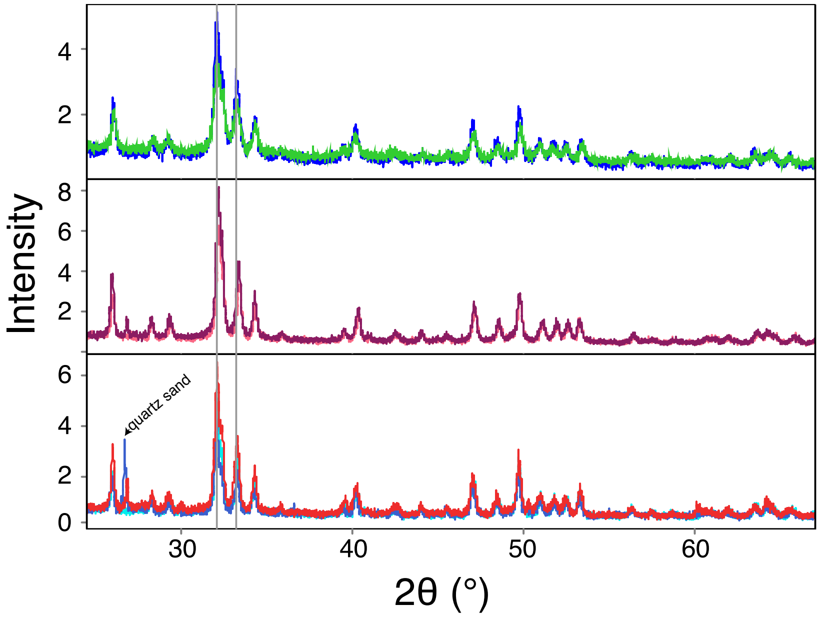

Figure 6.8: XRD data for modern and ancient inarticulate brachiopod samples. top, Modern cleaned and powdered samples of *Glottidia albida* from the San Pedro shelf off Newport Bay, CA (green) and *Lingula unguis* from Polillo Islands, Philippines (blue). middle, two separate cleaned and powdered samples of *Lingula sp.* from the Decorah Formation (purple and pink). bottom, cleaned and powdered samples of *Lingula sp.* from the *Crepicephalus* zone of the Eau Claire Formation near Strum, WI (light blue and dark blue) and Colfax, WI (red).

Three separate prepared samples yielded clumped isotope temperatures on the Strum, WI inarticulate brachiopods of 26° ± 2°C, 30° ± 3°C (n=2) and 34° ± 6°C. The average for all analyses from Strum, WI is 30° ± 2°C. One prepared sample from the Colfax, WI site yielded a clumped isotope temperature of 41° ± 0.5°C (n=3). While, the Eau Claire Formation is very carbonate lean, a sample of the carbonate matrix of the Upper Cambrian St. Lawrence Formation from a nearby location was analyzed and yielded a clumped isotope temperature of 48° ± 6°C. The average calculated $\delta^{18}O_{water}$ for the Strum, WI samples, assuming an equilibrium relationship that follows calcite [24], is -3.6 ± 0.5‰ VSMOW. The calculated $\delta^{18}O_{water}$ composition for the Colfax, WI site is -1.7 ± 0.1‰ VSMOW.

6.6 Discussion

6.6.1 Diagenetic alteration

The petrography and elemental analysis suggests the variability of clumped isotopic values from a single location can be directly related to degree of recrystallization. A range of clumped isotope data from the Late Ordovician and early Silurian suggests a pattern of diagenesis that relates clumped isotope temperature to trace metal incorporation into shell materials (Fig. 6.9) [28, 29]. This pattern falls apart for the older Decorah, Volkhov, Asery and Kunda formations despite similar and even lower clumped isotope temperatures (Fig. 6.9). A possible explanation for this difference is the importance in sedimentation rate on both proxies. Fossil materials from depositional environments with very high sedimentation rates that result in thick overburdens like the passive margin along western Laurentia have extremely high clumped isotope temperatures and high trace metal incorporation (Table 6.1). Fossil materials from depositional environments with moderate sedimentation rates resulting in maximum overburdens of 3–4 km, have low temperature end-members with little evidence for recrystallization and very low trace metal incorporation. These environments also have some materials with elevated clumped isotope temperatures including sparry calcite cements with higher trace metal incorporation (Table 6.1 and Fig. 6.9). Fossil materials from depositional environments with very low sedimentation rates and the thinnest overburden like the cratonic Volkhov and Decorah formations have low clumped isotope temperature end-members with little evidence for recrystallization but the trace metal enrichments do not suggest well-preserved fossil materials (Table 6.1 and Fig. 6.9).

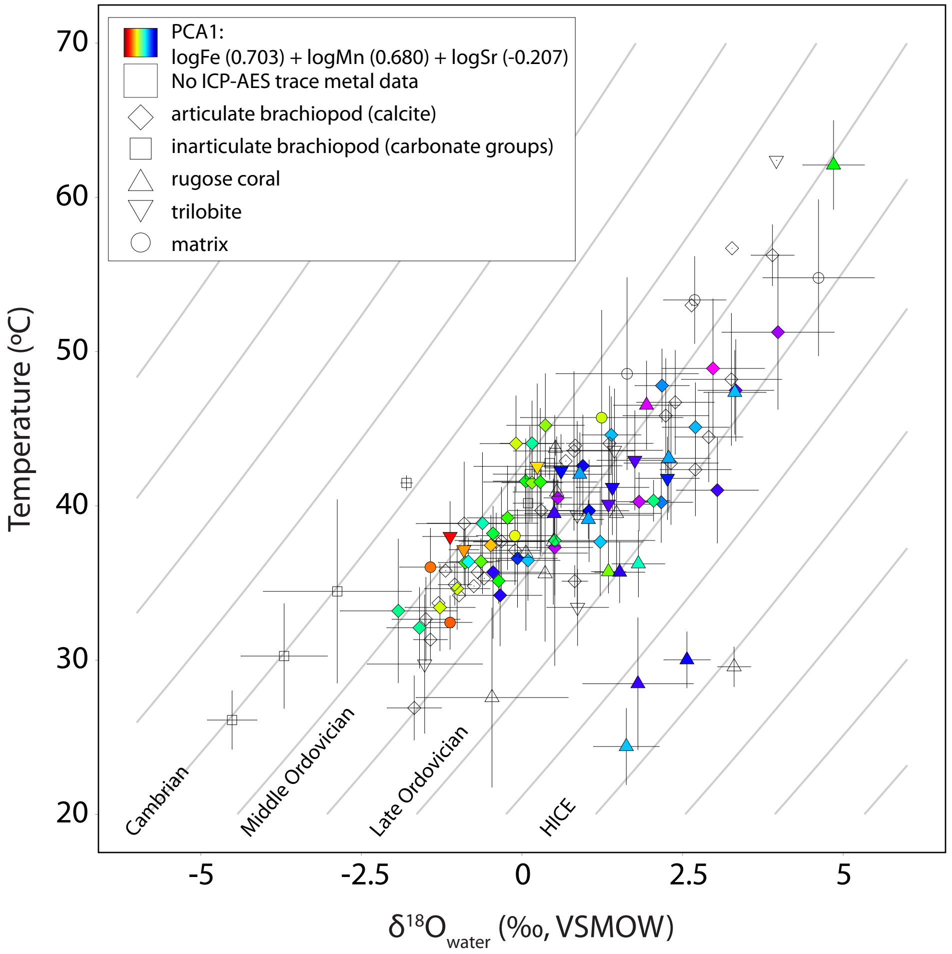

Figure 6.9: Cross plot of clumped isotope temperature vs $\delta^{18}O_{water}$. Grey lines are constant $\delta^{18}O_{min}$. The PCA1 of trace metals abundances of Fe, Mn and Sr is plotted for the calcitic taxa that have been analyzed.

In these settings, there is abundant sedimentological evidence for early seafloor mineralization including abundant hardgrounds, phosphatized grains and iron ooids. These results reinforce the importance of using a wide range of methods including petrographic and elemental analyses particularly on the micro-scale to characterize the diagenetic alteration of materials analyzed using carbonate clumped isotope thermometry. However, the promise this combined approach holds is a better understanding of the isotopic data used to make paleoclimate reconstructions.

Location	Minimum T (°C)	Maximum T (°C)	Margin Type	Sedimentation Rate	Trace Metal Behavior
Nevada	100	215	Passive Margin	Very High	Useful
Cincinnati Series	29	62	Cratonic	Moderate	Useful
Anticosti Island	24	56	Foreland Basin	Moderate	Useful
Decorah Formation	27	46	Cratonic	Low	early mineralization
Volkhov Formation	32	41	Cratonic	Low	early mineralization

Table 6.1: Clumped isotope temperature range and trace metal results for Ordovician fossils recovered from a range of burial environments

6.6.2 Phosphate-calcite equilibrium precipitation

The combined measurements of clumped isotope temperature and δ^{18}O of the CO_3 groups substituted into the phosphate lattice of inarticulate brachiopods paired with the $\delta^{18}O_{PO4}$ can be used to test whether these two phases both precipitated in equilibrium from the same fluid. There are two complicating factors in interpreting these results. First, some have suggested the $\delta^{18}O_{PO4}$ in inarticulate brachiopods is in part set by a contribution from the isotopic composition of the organic phosphate groups. Studies that recover high-resolution variability across laminae refute the importance of this oxygen source, suggesting that climatic variations are recorded in the $\delta^{18}O_{PO4}$ [54]. Additionally, the state of the water-phosphate mineral equilibrium relationship is currently in a state of flux with at least five widely used equilibrium fractionation equations present in the literature [55, 56, 57, 6, 5]. These five equilibrium fractionation equations can be compared using data from this study (Table 6.2). The two most recent phosphate-water equilibrium reactions based on results using the Ag_3PO_4 precipitation method, [6, 5] suggest the carbonate and phosphate in the fossil materials were precipitated in equilibrium and [5] indicates the carbonate and phosphate of all of the materials including the modern calibration materials were precipitated in equilibrium. The most recent equation from [5] is potentially biased to achieve this result because it was constructed based on presumed equilibrium between CO_3 and PO_4 measurements [5].

ID	n	δ^{13}C (PDB)	$\delta^{18}O_{min}$ (PDB)	Δ_{47} IL	T IL (°C)	Δ_{47} URF	T URF (°C)	$\delta^{18}O_w$ (VSMOW)	$\delta^{18}O_{PO4}$ (VSMOW)	C1	C2	C3	C4	C5
CIB	3	-4.61	-7.27	0.571	46.4	0.640	40.0	-2.1	16.70	0.10	0.10	-0.48	-2.02	-1.9
ECIB	4	-5.02	-7.06	0.612	34.1	0.676	29.5	-3.9	16.10	-2.94	-2.94	-3.59	-4.94	-5
DIB	7	-1.59	-5.28	0.572	46.3	0.640	40.2	-0.1	17.50	0.95	0.95	0.37	-1.17	-1.1
PIIB	5	-4.27	-1.10	0.613	33.9	0.683	27.9	1.9	20.50	1.08	1.08	0.43	-0.90	-1
PIIB*	-						28.5*	0.1*	20.50	1.22	1.22	0.57	-0.77	-0.9
TIIB*	-						16.8*	-0.5*	21.40	-0.60	-0.60	-1.31	-2.46	-2.8

Table 6.2: Comparison of calculated $\delta^{18}O_{water}$ compositions using the clumped isotope temperatures and $\delta^{18}O_{CO3}$ and $\delta^{18}O_{PO4}$ measurements for a range of PO_4–H_2O equilibrium equations (C1–C5, see below for references). The last two samples with a * are re-calculated based on the mean annual temperature measurements and nearby $\delta^{18}O_{water}$ measurements using only the $\delta^{18}O_{PO4}$ measurement.

C1 [55], C2 [56], C3 [57], C4 [6], C5 [5]

6.6.3 Climate of the Cambrian and Ordovician

The results from this study and previous studies using carbonate clumped isotope thermometry provide a consistent picture of the climate of the Cambrian and Ordovician (Fig. 6.10) [28, 29]. The petrographic and elemental analyses completed as a component of the clumped isotope studies indicate that a small amount of reprecipitated carbonate is a component of most or all samples analyzed. Despite similar $\delta^{18}O_{min}$ measurements for a given sample site, these inclusions are likely responsible for the range in temperatures measured. Thus, the most conservative temperature estimate for each site is represented by the lowest reproducible clumped isotope temperature. Using this interpretation of the datasets for the Cambrian and Ordovician, this would suggest temperatures within the broad epeiric seas that dominate the sedimentologic record of this interval were warm—35°C for the Early Silurian, Middle and End-Ordovician, 27°C during the HICE associated with the End-Ordovician Glaciation, 32°C for the Early Ordovician and 30°C for the Late Cambrian. While most of the sites analyzed sat at or near the equator, the Early Ordovician Russian stratigraphy was likely slightly further south. These temperatures are equal to or slightly warmer than the modern West Pacific warm pool when there is still significant ice at the poles. They are also within the range estimated by some climate modelers for equatorial sea surface temperatures during the ice-free Eocene Climatic Optimum [58]. These results suggest it will be helpful to continue to explore and constrain the full temperature range of the Earth's climatic system during ice-free, greenhouse conditions.

While the resolution of clumped isotope data on fossil materials is not yet high enough to fully test the importance of temperature on the evolutionary trends in the Cambrian and Early Ordovician, currently the data does not support a temperature decline as large as previously estimated from conodont phosphate analyses [1] over this interval. This suggested temperature decrease was described as a forcing mechanism for the Early Ordovician radiation of skeletal animals [1], however the limited clumped isotope data do not support a significant temperature decline associated with the Ordovician Radiation.

6.6.4 Seawater δ^{18}O through time

The clumped isotope data generated from Cambrian- and Ordovician-aged strata span a period when the $\delta^{18}O_{min}$ declines from 0‰ during the end-Ordovician glaciation to -7 ‰ by Cambrian time(Fig. 6.10). The calculated $\delta^{18}O_{water}$ compositions from this study and previous studies indicate the isotopic composition over the Ordovician largely reflects changes in ice volume related to the end-Ordovician

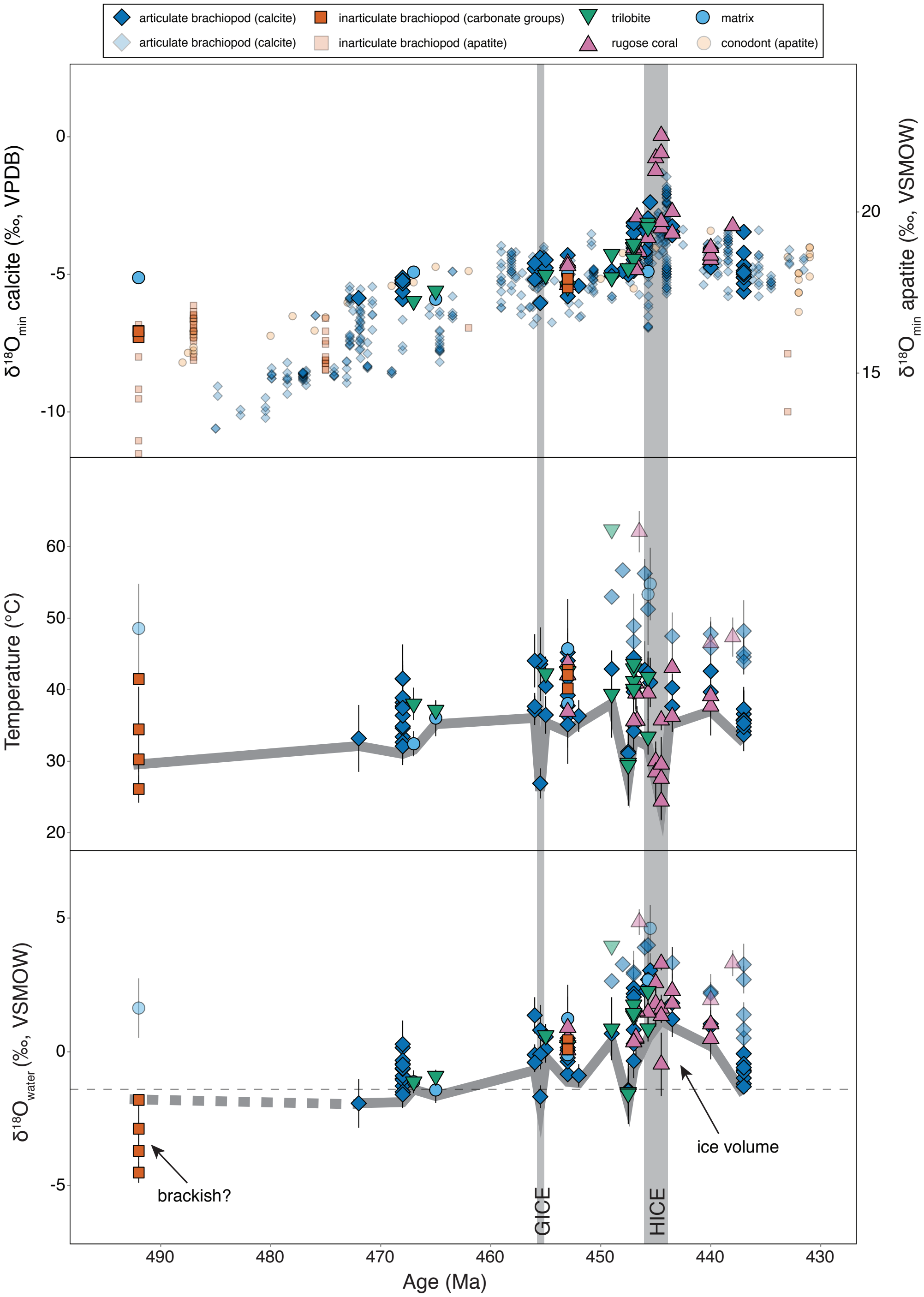

Figure 6.10: $\delta^{18}O_{min}$, clumped isotope temperature and calculated $\delta^{18}O_{water}$ for the Cambrian and Ordovician.

glaciation. The early Ordovician data from Russia yield values predicted for ice free conditions. While, the lowest temperatures from the Cambrian-aged Eau Claire Formation suggest more depleted fluid compositions (-3‰), a variety of observations suggest these coarse grained near shore sandstones may have been brackish. Using the temperatures measured from the Wisconsin inarticulate brachiopods to estimate the fluid composition in equilibrium with the $\delta^{18}O_{CO3}$ from the inarticulate brachiopods of the same age from the more distal Iowa sections, suggests $\delta^{18}O_{seawater}$ values of ~ 0‰ [40, 43]. Results presented here are in agreement with ophiolite studies that show no change in $\delta^{18}O_{seawater}$ over Earth's history [15, 16].

The results from this study indicate that diagenesis is likely an important process that accounts for a significant amount of the variability in the $\delta^{18}O_{min}$ record. The burial history of each of the calcitic and phosphatic taxa used to create the record, particularly from the earliest Ordovician and Cambrian when the record is scarce, are important to constrain. There is a visible offset between the calcite $\delta^{18}O$ and phosphate $\delta^{18}O$ from the literature in the Cambrian and Early Ordovician when the two datasets are aligned in the Middle-Late Ordovician (Fig. 6.10, light points in upper panel).

6.7 Conclusions

A long-term debate focused on the mirrored decline in $\delta^{18}O_{min}$ of carbonate, apatite and chert has generated two end-member hypotheses 1) a change in the bulk isotopic of seawater through time to values approaching -7‰ in the Cambrian or 2) a record that is largely controlled by warmer temperatures in the past. The ability to deconvolve fluid composition from temperature using clumped isotope thermometry provides an approach to interpret the long-term $\delta^{18}O_{min}$ records of carbonate and apatite. Results from Ordovician and Cambrian calcitic and phosphatic taxa indicate the $\delta^{18}O_{seawater}$ did not reach values as light as -7‰. The Eau Claire samples indicate that it was at most -3‰ however, our preferred interpretation is that these samples were more depleted in δ^{18}O because they lived in a brackish environment. Instead, by constraining the relative effect of diagenetic recrystallization on the materials analyzed, the equatorial climate of the Ordovician and Cambrian appears to be slightly warmer on average than today.

"What did one brachiopod say to the other brachiopod? Nothing, he was inarticulate."

6.8 Acknowledgements

Leonid Popov provided brachiopod samples of the Volkhov Formation and the Los Angeles County Museum of Natural History and Waikiki Aquarium provided samples of modern inarticulate and calcitic brachiopods. Nigel Hughes, Matthew Robles and Gerry Gunderson for providing materials and collaborating on fieldwork in the Eau Claire Formation. Seth Finnegan, Norlene Emerson, Clint Cowan, and Pat McLaughlin provided invaluable assistance on the Decorah Formation in the field. Nami Kitchen, Joel Hurowitz, Chi Ma, Daniel Stolper, Renata Cummins, and Katie Eiler assisted with analytical measurements and method development. We would also like to thank Magali Bonifaci for providing the high temperature dolomite calibration dataset used as part of our calibration line. Ken MacLeod is responsible for $\delta^{18}O_{PO4}$ measurements on splits of the ancient inarticulate brachiopod samples and two of our modern inarticulate samples. A National Science Foundation Graduate Research Fellowship was provided to K. Bergmann. W. Fischer acknowledges support from the Agouron Institute and a David and Lucile Packard Fellowship for Science and Engineering.

References

[1] J.A. Trotter. Did cooling oceans trigger Ordovician biodiversification? evidence from conodont thermometry. *Science*, 321(5894):1295–1295, 2008.

[2] J.B.D. Jaffres, G.A. Shields, and K. Wallmann. The oxygen isotope evolution of seawater: A critical review of a long-standing controversy and an improved geological water cycle model for the past 3.4 billion years. *Earth-Science Reviews*, 83(1-2):83–122, 2007.

[3] J.F. Kasting. Earth sciences - ups and downs of ancient oxygen. *Nature*, 443(7112):643–+, 2006.

[4] J. Veizer, D. Ala, K. Azmy, P. Bruckschen, D. Buhl, F. Bruhn, G.A.F. Carden, A. Diener, S. Ebneth, Y. Godderis, T. Jasper, C. Korte, F. Pawellek, O.G. Podlaha, and H. Strauss. Sr-87/Sr-86, delta C-13 and delta O-18 evolution of Phanerozoic seawater. *Chemical Geology*, 161(1-3):59–88, 1999.

[5] C. Lecuyer, R. Amiot, A. Touzeau, and J.A. Trotter. Calibration of the phosphate delta o-18 thermometer with carbonate-water oxygen isotope fractionation equations. *Chemical Geology*, 2013.

[6] E. Puceat, M.M. Joachimski, A. Bouilloux, F. Monna, A. Bonin, S. Motreuil, P. Moriniere, S. Henard, J. Mourin, G. Dera, and D. Quesne. Revised phosphate-water fractionation equation reassessing paleotemperatures derived from biogenic apatite. *Earth and Planetary Science Letters*, 298:135–142, 2010.

[7] S. Epstein, E. Degens, and D.L. Graf. Oxygen isotopic compositions of coexisting calcite and dolomite. *Journal of Geophysical Research*, 67:1636, 1962.

[8] A. Shemesh, Y. Kolodny, and B. Luz. Oxygen isotope variations in phosphate of biogenic apatites .2. phosphorite rocks. *Earth and Planetary Science Letters*, 64(3):405–416, 1983.

[9] J. Karhu and S. Epstein. The implication of the oxygen isotope records in coexisting cherts and phosphates. *Geochimica Et Cosmochimica Acta*, 50(8):1745–1756, 1986.

[10] L.P. Knauth and S. Epstein. Hydrogen and oxygen isotope ratios in nodular and bedded cherts. *Geochimica Et Cosmochimica Acta*, 40:1095–1108, 1976.

[11] M.M. Joachimski, R. van Geldern, S. Breisig, W. Buggisch, and J. Day. Oxygen isotope evolution of biogenic calcite and apatite during the Middle and Late Devonian. *International Journal of Earth Sciences*, 93(4):542–553, 2004.

[12] B. Wenzel, C. Lecuyer, and M.M. Joachimski. Comparing oxygen isotope records of Silurian calcite and phosphate - delta O-18 compositions of brachiopods and conodonts. *Geochimica Et Cosmochimica Acta*, 64(11):1859–1872, 2000.

[13] A. Shemesh, Y. Kolodny, and B. Luz. Isotope geochemistry of oxygen and carbon in phosphate and carbonate of phosphorite francolite. *Geochimica Et Cosmochimica Acta*, 52(11):2565–2572, 1988.

[14] D. Bassett, K.G. Macleod, J.E. Miller, and R.L. Ethington. Oxygen isotopic composition of biogenic phosphate and the temperature of early Ordovician seawater. *Palaios*, 22(1):98–103, 2007.

[15] K. Muehlenbachs and R. N. Clayton. Oxygen isotope composition of oceanic-crust and its bearing on seawater. *Journal of Geophysical Research*, 81(23):4365–4369, 1976.

[16] K Muehlenbachs. The oxygen isotopic composition of the oceans, sediments and the seafloor. *Chemical Geology*, 145(3-4):263–273, 1998.

[17] C. Holmden and K. Muehlenbachs. The O-18/O-16 ratio of 2-billion-year-old seawater inferred from ancient oceanic-crust. *Science*, 259(5102):1733–1736, 1993.

[18] H.D. Holland. The chemical evolution of the atmosphere and oceans. Princeton University Press, 1984.

[19] A. Prokoph, G.A. Shields, and J. Veizer. Compilation and time-series analysis of a marine carbonate delta O-18, delta C-13, Sr-87/Sr-86 and delta S-34 database through Earth history. *Earth-Science Reviews*, 87(3-4):113–133, 2008.

[20] J. Veizer, P. Bruckschen, F. Pawellek, A. Diener, O.G. Podlaha, G.A.F. Carden, T. Jasper, C. Korte, H. Strauss, K. Azmy, and D. Ala. Oxygen isotope evolution of Phanerozoic seawater. *Palaeogeography Palaeoclimatology Palaeoecology*, 132(1-4):159–172, 1997.

[21] E. Puceat, M. Joachimski, A. Bonin, S. Motreuil, F. Monna, A. Bouilloux, D. Quesne, P. Moriniere, and J. Mourin. Revised delta O-18 phosphate-water fractionation equation from fish raised in controlled environment. *Geochimica Et Cosmochimica Acta*, 73(13):A1058–A1058, 2009.

[22] J.M. Eiler. "clumped-isotope" geochemistry - the study of naturally-occurring, multiply-substituted isotopologues. *Earth and Planetary Science Letters*, 262(3-4):309–327, 2007.

[23] I. Freidman and J.R. O'Neil. Compilation of stable isotope fractionation factors of geochemical interest. Technical report, 1977.

[24] S.T. Kim and J.R. Oneil. Equilibrium and nonequilibrium oxygen isotope effects in synthetic carbonates. *Geochimica Et Cosmochimica Acta*, 61(16):3461–3475, 1997.

[25] R. Eagle, E. Schauble, A. Tripati, T. Tutken, H. Fricke, R. Hulbert, and J. Eiler. 'clumped isotope' thermometry in bioapatite. *Geochimica Et Cosmochimica Acta*, 74(12):A256–A256, 2010.

[26] R.A. Eagle, E.A. Schauble, A.K. Tripati, T. Tutken, R.C. Hulbert, and J.M. Eiler. Body temperatures of modern and extinct vertebrates from C-13-O-18 bond abundances in bioapatite. *Proceedings of the National Academy of Sciences of the United States of America*, 107(23):10377–10382, 2010.

[27] G.A. Schmidt, G.R. Bigg, and E.J Rohling. Global seawater oxygen-18 database - v1.21. *Geochimica Et Cosmochimica Acta*, 1999.

[28] S. Finnegan, K. Bergmann, J.M. Eiler, D.S. Jones, D.A. Fike, I. Eisenman, N.C. Hughes, A.K. Tripati, and W.W. Fischer. The magnitude and duration of Late Ordovician-Early Silurian glaciation. *Science*, 331(6019):903–906, 2011.

[29] R.E. Came, J.M. Eiler, J. Veizer, K. Azmy, U. Brand, and C.R. Weidman. Coupling of surface temperatures and atmospheric CO2 concentrations during the Palaeozoic era. *Nature*, 449(7159):198–U193, 2007.

[30] N.R. Emerson. *Sedimentology, Sequence Stratigraphy, and Brachiopod Biostratigraphy of the Ordovician (Mohawkian) Decorah Formation, Midcontinent, USA*. Ph.D. thesis, 2002.

[31] J.A. Simo, N.R. Emerson, C.W. Byers, and G.A. Ludvigson. Anatomy of an embayment in an Ordovician epeiric sea, Upper Mississippi Valley, USA. *Geology*, 31(6):545–548, 2003.

[32] N.R. Emerson, J.A. Simo, C.W. Byers, and J. Fournelle. Correlation of (Ordovician, Mohawkian) K-bentonites in the upper Mississippi Valley using apatite chemistry: implications for stratigraphic interpretation of the mixed carbonate-siliciclastic Decorah Formation. *Palaeogeography Palaeoclimatology Palaeoecology*, 210(2-4):215–233, 2004.

[33] G.A. Ludvigson, B.J. Witzke, L.A. Gonzalez, S.J. Carpenter, C.L. Schneider, and F. Hasiuk. Late Ordovician (Turinian-Chatfieldian) carbon isotope excursions and their stratigraphic and paleoceanographic significance. *Palaeogeography Palaeoclimatology Palaeoecology*, 210(2-4):187–214, 2004.

[34] W. Buggisch, M.M. Joachimski, O. Lehnert, S.M. Bergstrom, J.E. Repetski, and G.F. Webers. Did intense volcanism trigger the first Late Ordovician icehouse? *Geology*, 38(4):327–330, 2010.

[35] T. Tolmacheva, E. Egerquist, T. Meidla, O. Tinn, and L. Holmer. Faunal composition and dynamics in unconsolidated sediments: a case study from the middle Ordovician of the East Baltic. *Geological Magazine*, 140(1):31–44, 2003.

[36] E. Egerquist. New brachiopods from the Lower-Middle Ordovician (Billingen-Volkhov stages of the East Baltic. *Acta Palaeontologica Polonica*, 48(1):31–38, 2003.

[37] A.V. Dronov, T. Tolmacheva, and E. Raevskaya. Cambrian and Ordovician of St. Petersburg Region. *6th Baltic Stratigraphical Conference*, pages 1–64, 2005.

[38] A.V. Dronov, J.V. Savitsky, P.V. Fedorov, and E.A. Tsyganova. Detailed lithostratigraphy of the Ordovician lower Volkhovian limestone along the eastern part of the Baltic-Ladoga Glint, northwestern Russia. *GFF*, 118(1):19–24, 2009.

[39] L.E. Popov, E. Egerquist, and M.A. Zuykov. Ordovician (Arenig-Caradoc) syntrophidine brachiopods from the Baltic Region. *Palaeontology*, 48(4):739–761, 2005.

[40] C.A. Cowan, D.L. Fox, A.C. Runkel, and M.R. Saltzman. Terrestrial-marine carbon cycle coupling in similar to 500-m.y.-old phosphatic brachiopods. *Geology*, 33(8):661–664, 2005.

[41] M.R. Saltzman, C.A. Cowan, A.C. Runkel, B. Runnegar, M.C. Stewart, and A.R. Palmer. The Late Cambrian SPICE (delta(13)c) event and the Sauk II-Sauk III regression: New evidence from Laurentian basins in Utah, Iowa, and Newfoundland. *Journal of Sedimentary Research*, 74(3):366–377, 2004.

[42] M. Elrick, S. Rieboldt, M. Saltzman, and R.M. McKay. Oxygen-isotope trends and seawater temperature changes across the Late Cambrian Steptoean positive carbon-isotope excursion (SPICE event). *Geology*, 39(10):987–990, 2011.

[43] T. Runkel. personal communication regarding the delta O-18 results from cowan et al., 2005. personal communication.

[44] P.L. Koch, N. Tuross, and M.L. Fogel. The effects of sample treatment and diagenesis on the isotopic integrity of carbonate in biogenic hydroxylapatite. *Journal of Archaeological Science*, 24(5):417–429, 1997.

[45] K.W. Huntington, J.M. Eiler, H.P. Affek, W. Guo, M. Bonifacie, L.Y. Yeung, N. Thiagarajan, B. Passey, A. Tripati, M. Daeron, and R. Came. Methods and limitations of 'clumped' CO2 isotope (Delta(47)) analysis by gas-source isotope ratio mass spectrometry. *Journal of Mass Spectrometry*, 44(9):1318–1329, 2009.

[46] B.H. Passey, N.E. Levin, T.E. Cerling, F.H. Brown, and J.M. Eiler. High-temperature environments of human evolution in East Africa based on bond ordering in paleosol carbonates. *Proceedings of the National Academy of Sciences of the United States of America*, 107(25):11245–11249, 2010.

[47] K.J. Dennis, H.P. Affek, B.H. Passey, D.P. Schrag, and J.M. Eiler. Defining an absolute reference frame for 'clumped' isotope studies of CO2. *Geochimica Et Cosmochimica Acta*, 75(22):7117–7131, 2011.

[48] G.A. Henkes, B. Passey, A.D. WaNamaker, E.L. Grossman, W.G. Ambrose, and M.L. Carroll. Carbonate clumped isotope compositions of modern marine mollusk and brachiopod shells. *Geochimica Et Cosmochimica Acta*, 106(1):307–325, 2013.

[49] M. Bonifaci and J. Eiler. High temperature dolomite calibration. inpress.

[50] P. Ghosh, J. Adkins, H. Affek, B. Balta, W.F. Guo, E.A. Schauble, D. Schrag, and J.M. Eller. C-13-O-18 bonds in carbonate minerals: A new kind of paleothermometer. *Geochimica Et Cosmochimica Acta*, 70(6):1439–1456, 2006.

[51] J. Rosenbaum and S.M.F. Sheppard. An isotopic study of siderites, dolomites and ankerites at high-temperatures. *Geochimica Et Cosmochimica Acta*, 50(6):1147–1150, 1986.

[52] N. Thiagarajan, W.F. Guo, J. Adkins, and J. Eiler. Clumped isotope calibration of modern deep sea corals and implications for vital effects. *Geochimica Et Cosmochimica Acta*, 73(13):A1324–A1324, 2009.

[53] A. Tripati, N. Thiagarajan, and J. Eiler. 'clumped isotope' thermometery in foraminifera. *Geochimica Et Cosmochimica Acta*, 72(12):A956–A956, 2008.

[54] D.L. Rodland, M. Kowalewski, D.L. Dettman, K.W. Flessa, V. Atudorei, and Z.D. Sharp. High-resolution analysis of delta O-18 in the biogenic phosphate of modern and fossil lingulid brachiopods. *Journal of Geology*, 111(4):441–453, 2003.

[55] A. Longinelli and S. Nuti. Revised phosphate-water isotopic temperature scale. *Earth and Planetary Science Letters*, 19(3):373–376, 1973.

[56] Y. Kolodny, B. Luz, and O. Navon. Oxygen isotope variations in phosphate of biogenic apatites .1. fish bone apatite - rechecking the rules of the game. *Earth and Planetary Science Letters*, 64(3):398–404, 1983.

[57] C. Lecuyer, P. Grandjean, and C.C. Emig. Determination of oxygen isotope fractionation between water and phosphate from living lingulids: Potential application to palaeoenvironmental studies. *Palaeogeography Palaeoclimatology Palaeoecology*, 126(1-2):101–108, 1996.

[58] M. Huber and L.C. Sloan. Heat transport, deep waters, and thermal gradients: Coupled simulation of an Eocene greenhouse climate. *Geophysical Research Letters*, 28(18):3481–3484, 2001.